Advanced Sensors and Instrumentation

Issue 16 • March 2022

ASI Program Update

Daniel Nichols
Department of Energy

Pattrick Calderoni
Idaho National Laboratory

The Advanced Sensors and Instrumentation (ASI) program has entered its 11th year since implementation in Fiscal Year (FY) 2011. The program has continued to show great resilience during the COVID-19 pandemic by producing remarkable accomplishments in the development of Instrumentation and Control (I&C) technologies, a portion of which are highlighted in this newsletter. Additionally, program elements have been able to make great strides in research and development (R&D) while under the Congressional budget continuing resolution, which has since concluded with the passage of the FY22 budget. While these past uncertainties have affected the program, ASI has demonstrated its adaptability and innovation while continuing to support the mission of the Department of Energy (DOE) and DOE Office of Nuclear Energy (NE). The ASI program continues its efforts towards the development and demonstration of mature technologies in response to stakeholder's needs which has been augmented by the technology gap analysis performed in during FY21.

The ASI program's Annual Review was held as a virtual webinar for 4 consecutive days in the fall of 2021 (November 15 - 18). It showcased 50 presentations from competitively awarded and directed research projects, including 7 Small Business Innovation Research (SBIR) awardees and 1 Industry Funding Opportunity Announcement (IFOA) awardee. These presentations provided a summary of accomplishments in FY 2021 and were organized into four research focus areas: Sensors for Advanced Reactors, Advanced Materials and Manufacturing Methods for Sensors Applications, Instrumentation for Irradiation Experiments, and Digital Technologies. The webinar had more than 120 attendees

Continued on next page

In this issue...

For more program information, including recent publications, please visit www.energy.gov/ne

U.S. DEPARTMENT OF ENERGY

Continued from previous page

from across the nuclear industry, national laboratories, universities, and government agencies.

Some additional accomplishments that were completed in FY 2021 include:

- An ASI website (https://asi.inl.gov/#/) has been developed and published that will serve as a repository of ASI program information on competitively awarded and directly-funded projects, annual summary reports, annual review webinar presentations, and bi-annual newsletters. Presentations, videos, poster presentations, along with links to relevant sites such as funding opportunities, are available.
- Three Consolidated Innovative Nuclear Research (CINR) projects led by DOE national laboratories and U.S. universities were awarded funding for FY 2021. These projects will conduct research focused on the performance of radiation-tolerant semiconductor materials such as gallium nitride, and gallium oxide, as well as the development and in-pile testing of real-time thermal conductivity monitoring technologies.
- Progress continues on the NE Sensor Database (https://nes.energy.gov/), which was created to collect, store, and maintain nuclear plant sensor technology information that would be easily accessed and queried on the web by the sensors and instrumentation user community. This sensor database will house relevant information regarding presently utilized sensors as well as clarification on needs and technology gaps necessary to be addressed.

Measurement of Macroscopic Radiation-Induced Changes in Optical Fiber

Sohel Rana
Idaho National Laboratory

Austin Fleming
Idaho National Laboratory

Introduction

Optical fiber technologies offer innovative measurement solutions that can potentially accelerate R&D activities and improve the competitiveness of advanced nuclear energy systems, since information transmitted via optical fiber is advantageous as a result of the fiber's low signal losses, wide bandwidth, immunity to electromagnetic induction effects, small and compact size. However, optical fiber undergoes optical properties changes in radiation fields, causing radiation-induced signal drift and leading to measurement errors in the physical parameters being sensed by optical-fiber-based sensors.

Radiation Effects on Optical Fibers

Intense radiation compacts the silica-based optical fiber, altering the fiber's refractive index (RI) and length. Radiation, primarily by attenuating and compacting the silica optical fibers, in many ways changes the optical, mechanical, and chemical properties of these fibers, thus affecting signal fidelity. Radiation-induced attenuation (RIA) increases the linear attenuation in silica-based fibers [1]. Different parameters govern the RIA levels and kinetics, and these parameters include the chemical compositions and manufacturing processes behind the fibers, the light-guiding properties of the fibers, the nature of the irradiation (e.g., x-ray, gamma ray, and neutron), the dose rate, the wavelength of the light used, the injected light power, and the irradiation temperature [1], [2]. On the other hand, radiation-induced compaction (RIC) causes structural changes in the fiber, leading to an overall density change [3]. While RIA leads to an RI change via the Kramer-Kronig relation [4], its determination is complex, and one must consider the spectrum over a wide frequency range [4]. RIC alters the RI through the Lorentz-Lorenz relation [5] and point dipole theory [6]. Until now, RIC has been calculated using various well-established and empirical equations. All these methods considered only the RIC when calculating radiation-induced RI/length changes. However, the RI and length may also change due to any specific phenomenon to which the fiber is subjected, including RIC, RIA, dopant diffusion, temperatures, stress relaxation of fiber, dose, and dose rate. In this regard, these methods fail to present the complete picture of radiation-induced changes in RI. As RI and length compaction are the input parameters for optical fiber sensors, accurate measurement of these parameters is crucial for predicting radiation's actual effects on optical fiber sensors, and for correcting sensor drift. Online measurement of radiation-induced changes in RI/length is a potential way of understanding structural changes in optical fiber exposed to a nuclear environment, thus aiding in the minimization of signal error.

Objective

The objective of this research is to measure radiation-induced macroscopic changes in optical fiber, using a simple optical-fiber-based cascaded Fabry-Perot interferometer (FPI). Compared to the conventional "cook-and-look" method, the analytical method based on the Lorentz-Lorenz relation, point dipole theory, etc., this technique offers unique features such as real-time determination of RI/length changes due to any specific phenomenon to which the fiber has been subjected, including RIC, RIA, dopant diffusion, stress relaxation of fiber, and temperatures. As a proof of concept to measure RI/length changes in optical fiber, we experimentally demonstrated real-time monitoring of temperature's effect on RI/length and used the cascaded FPI to measure the fiber's thermo-optic coefficient (TOC) and thermal expansion coefficient (TEC).

Current Status

Figure 1 shows the design architecture of the cascaded FPI for the measurement of RI/length changes in silica optical fiber. It consists of an air cavity (hollow) and a silica cavity (solid) contained within the same fiber (Fig. 1[a]). The air cavity is used to monitor the temperature-induced changes in cavity length, whereas the silica cavity can be used to measure the RI, using knowledge of optical science. To fabricate the cascaded FPI, simple cleaving and splicing processes were applied. As a first step, the single-mode fiber, capillary tube, and coreless (CL) fiber were cleaved using a cleaving tool (Fig. 1[b]), and then a fusion splicer was used to fusion splice the SMF-28 with the capillary tube (Fig. 1[c]). Next, a linear stage was used in conjunction with the cleaving tool to cleave the spliced capillary at a distance from the splicing point (Fig. 1[c]). A CL fiber was cleaved and spliced with the capillary tube to complete the air cavity (Fig. 1[d]). The CL fiber was chosen for the silica cavity in order to obtain information about the pure silica optical fiber. To construct the silica cavity, the CL fiber was cleaved at a distance from the point where

Continued on next page

Continued from previous page

the capillary and CL fiber had been spliced (Fig. 1[d]). A microscopic image of the fabricated cascaded FPI is shown in Fig. 1(e).

The fabricated cascaded FPI structure's measurements of the temperature-induced length variation in the air cavity, along with the RI variation in the silica cavity, are shown in Fig. 2(a) and (b), respectively. The measured TEC and TOC of the silica optical fiber are 5.53×10^{-7}/°C and 4.28×10^{-6}/°C, respectively, which is in good agreement with the value given in the literature value. Since the cascaded FPI can successfully monitor real-time RI/length changes in optical fiber, it is expected to also be able to measure those parameters in a radiation environment.

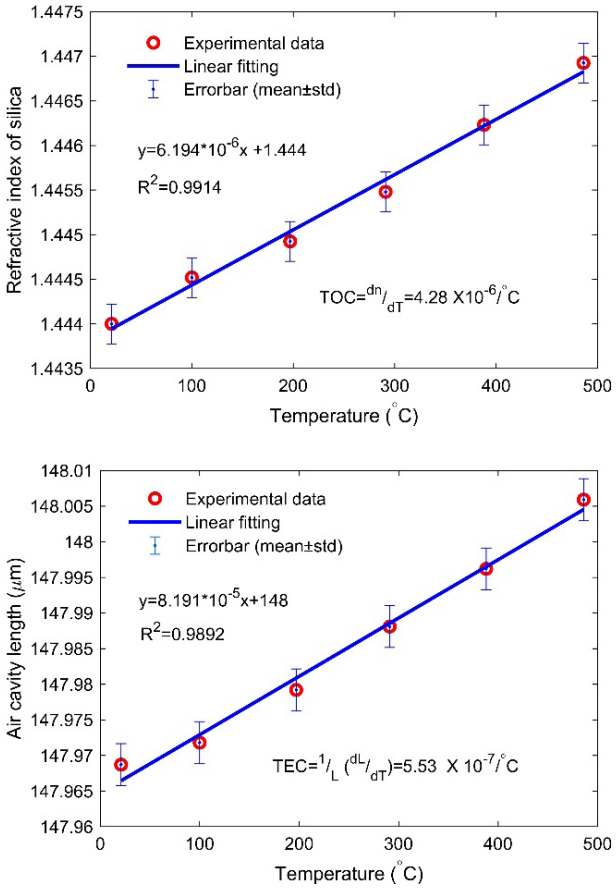

Figure 2. Real-time measurement of the temperature-induced changes in the silica optical fiber's TEC (top) and TOC (bottom)

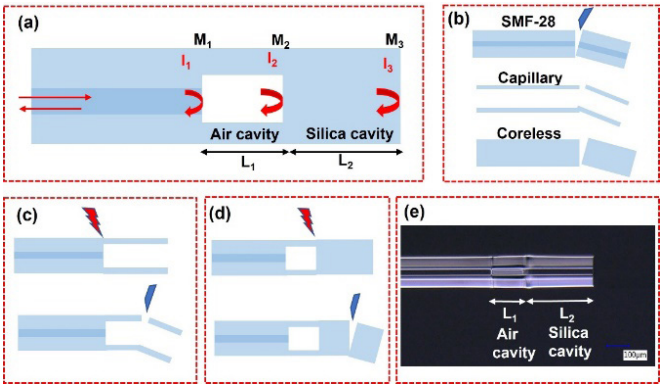

Figure 1. Schematic and fabrication process for the cascaded FPI: (a) schematic of the cascaded FPI, (b) cleaving of required fibers and capillary, (c, d) splicing and cleaving steps, and (e) microscopic image of the fabricated cascaded FPI.

Impact and Applications in the Nuclear Field

With applications of fiber optic technologies gradually penetrating into the nuclear field, the largest contribution to the nuclear community is expected to be the development of instrumentation to support the creation, testing, and qualification of nuclear fuels and materials. Research on fiber-optic-based systems will create opportunities for other measurement capabilities for in-pile instrumentation. It will also benefit the nuclear science community, as well as the scientific community at large.

References

[1] S. Girard et al., "Radiation Effects on Silica-Based Optical Fibers: Recent Advances and Future Challenges," IEEE Transactions on Nuclear Science, vol. 60, no. 3, pp. 2015–2036, Jun. 2013.

[2] S. Girard et al., "Recent advances in radiation-hardened fiber-based technologies for space applications," J. Opt., vol. 20, no. 9, p. 093001, Aug. 2018.

[3] W. Primak and R. Kampwirth, "The Radiation Compaction of Vitreous Silica," Journal of Applied Physics, vol. 39, no. 12, pp. 5651–5658, Nov. 1968.

[4] D. C. Hutchings, M. Sheik-Bahae, D. J. Hagan, and E. W. Van Stryland, "Kramers-Krönig relations in nonlinear optics," Opt Quant Electron, vol. 24, no. 1, pp. 1–30, Jan. 1992.

[5] S. Rana, H. Subbaraman, A. Fleming, and N. Kandadai, "Numerical Analysis of Radiation Effects on Fiber Optic Sensors," Sensors, vol. 21, no. 12, Art. no. 12, Jan. 2021.

[6] S. Rana, A. Fleming, N. Kandadai, and H. Subbaraman, "Active Compensation of Radiation Effects on Optical Fibers for Sensing Applications," Sensors, vol. 21, no. 24, Art. no. 24, Jan. 2021.

High-Temperature Irradiation-Resistant Thermocouple (HTIR-TC) Qualification Work

Richard Skifton
Idaho National Laboratory

Introduction

The high-temperature irradiation-resistant thermocouple (HTIR-TC) has successfully passed through the design, calibration, and qualification phases, following the guidelines for sensors developed under the Nuclear Energy Enabling Technologies (NEET) Advanced Sensors and Instrumentation program [1]. The qualification test needs were laid out in a qualification document [2], and the HTIR-TC underwent in-reactor testing for over a year in the Advanced Test Reactor (ATR)'s high-neutron-flux (a perturbed thermal flux of up to ~2.8×10^{14} nv and a fast flux of up to ~2.25×10^{14} nv), high-temperature (up to 1550°C) environment as part of the Advanced Gas Reactor (AGR) 5/6/7 fuel test. In this test, several HTIR-TCs were placed at various locations in the test fixture, which was designed for evaluating the performance of new advanced fuels designed specifically for the AGR program.

The following is an overview of how the HTIR-TCs followed the qualification guidelines and processes [1], their performance results from the aforementioned reactor qualification test, and their performance features, including measurement range, accuracy, repeatability, drift, and end of life (EOL).

Qualification Guidelines and Processes

The qualification guidelines for instrumentation developed at Idaho National Laboratory (INL) [1] are based on accepted procedural and quality assurance standards for product development. They are intended as a useful resource for INL instrumentation R&D by referencing and consolidating guidelines pertaining to NASA, Nuclear Quality Assurance (NQA)-1, International Organization for Standardization metrology, and nuclear industry standards in a manner pertinent to INL's sensor system development process.

The overall product development and quality assurance processes described in the qualification guidelines are divided into three main phases:

- Design Phase
- Calibration Phase
- Qualification Phase.

HTIR-TC Performance Demonstration in the ATR

Construction and calibration of the HTIR-TCs used in the AGR-5/6/7 test followed the guidelines presented in the preliminary build and calibration reports, as well as specific controlled documents pertaining to each build [3-5]. Furthermore, the performance requirements were based on the function and operation requirements report [6].

Of the five capsules in AGR 5/6/7, only capsules 1 and 3 contained installed HTIR-TCs for measuring experimental temperatures. However, the lead wires for each TC needed to exit the reactor core by passing through designated channels in the upper capsules. This means, for example, that the HTIR-TCs positioned for temperature measurement in capsule 1 had to pass through the high-thermal-neutron-flux regions of the reactor core reflected in capsule 3 (i.e., the reactor height midplane). Thus, although the HTIR-TCs in capsule 1 measured a lower temperature (as expected), the drift caused by thermal- and fast-neutron-flux-induced changes in the cable thermoelements would be similar for every TC located in capsules 1 and 3.

The test fixture also had provision to pass a small adjustable He-Ne mixture gas flow around the TCs in order to maintain a constant temperature and minimize the effect of power fluctuations on the TC temperature readings [7].

The gas flow was maintained at a minimal value and did not remove heat via convection. It merely provided a high thermal conduction path to the cooler high water flow of the reactor coolant outside the capsule housing serving as a heat sink for the capsule.

HTIR-TC Drift Model

Generally speaking, all TC types eventually drift after use. There are two major sources of TC drift during irradiation tests: temperatures exceeding design parameters and thermoelement transmutation. Both have been modeled to capture the apparent drift seen in AGR 5/6/7. Regarding high-temperature drift, it was observed, even in out-of-pile testing, that HTIR-TCs drift when temperatures approach within 400°C of the heat treatment and calibration temperatures. With thermoelement transmutation, the thermal neutron flux is captured by the thermoelements in the TC, resulting in signal drift.

A common misconception about TC sensors is that the temperature measurement is generated in the junction

Continued on next page

Continued from previous page

Table 1. Comparison of the calculated and the observed HTIR-TC drifts in the ATR test.

HTIR-TC #	Time at High Temperature (EFPD)	Operating Temperature [°C]	Drift Calculated by HTIR-TC Drift Model [%]	Observed Drift of HTIR-TC in ATR Test [%]	Difference between Calculated and Observed Drift [%]
1-12	125	1293	-3.29	-3.33	~ -0.03
1-13	125	1293	-3.29	-3.33	~ -0.03
1-14	125	1381	-3.50	-3.48	~ 0.02
3-5	125	1500	-8.65	-8.67	~ -0.02

(i.e., where dissimilar wires are joined together). In actuality, however, the EMF is generated in the length of thermoelement.

Concerning the effect that the two sources of drift had on the HTIR-TC cable during the AGR 5/6/7 test, both were modeled and summed so that the calculated drift could be compared to the observed drift, as shown in Table 1. The empirical model, which extends out over 125 effective full-power days (EFPD) aligns with what was observed over the same duration for the four HTIR-TCs installed in AGR 5/6/7. The localized temperature over the actual length of the HTIR-TC cable was utilized from the experiment model [8].

Table 2. Summary of HTIR-TC general requirements.

Parameter	Requirement	Measured
Temperature Range Min [°C] Max [°C]	Room Temp 1550	Room Temp 1550
Accuracy [%]	±1	±0.4 >100 ±1 <100
Repeatability [%]	±1	<±0.3
Total drift in ATR [%]	-3.5	-3.5[2]
Drift[3] in BWR/PWR [%]	-1	-0.86[2]
Thermal Transients[4]	10	14 – 19

[1]For 125 EFPDs of exposure when operating at less than the heat treatment temperature
[2]Calculated from drift model
[3]For 18-month refueling cycle.
[4]Greater than 50°C/hour.

Conclusions

Based on the HTIR-TC drift model and the results of the HTIR-TC qualification test, in which the TCs were installed as part of the AGR 5/6/7 experimental test fixture, the present HTIR-TC design should be considered qualified for the following three applications:

1. Standalone TC in a well-moderated commercial power reactor (i.e., a boiling-water reactor [BWR] or pressurized-water reactor [PWR]), used for measuring reactor temperatures of <1050°C throughout a full 18-month refueling interval, as long as the temperature change during normal startup/shutdown is controlled and kept below ~50°C/hour. The drift for this application (using the conservative HTIR-TC neutron absorption coefficient of ~2.3 barns) is expected to be <0.9%. Because the HTIR-TC is really designed to measure high temperatures, it is unlikely to be used as the primary temperature sensor, but as a back-up sensor for monitoring the commercial power reactor inlet and outlet temperatures that could result if there was a loss of coolant accident.

Note that the 1050°C value is >650°C higher than the core outlet temperature for these reactors, and well below the heat treatment temperature of the HTIR-TCs. In this application, the HTIR-TC can, in the event of an accident, also be used to measure core temperatures of up to ~1550°C for a short period (i.e., approximately 1200 hours) before the reactor is shut down and the temperature cools, without entailing any drift concerns during the presumably short duration of this high-temperature transient. There have already been several cases in which NPPs have made inquiries regarding the use of HTIR-TCs.

2. Standalone TC in any commercial non-nuclear facility, used for measuring temperatures of <1050°C over a prolonged period. The drift for this application should be <0.5%, since drift does not stem from neutron fluence effects. Accurate measurements should also be possible at up to 1550°C for at least a short time (i.e., approximately 1200 hours) during high-temperature transients. As with the previous application, the temperature change during normal startup or shutdown should be kept below ~50°C/hour.

3. TC in a test fixture for conducting fuel experiment tests in a test reactor (e.g., the ATR). For such applications, if the max temperature is controlled to within 1%, temperature measurements of up to 1550°C are feasible over a period of 125 EFPDs, with a drift of <4% when the peak thermal flux is ~2.8×10^{14} nv and the fast flux is ~2.3×10^{14} nv. Also, provisions should be made for accurate temperature and neutron flux profile calculations and/or measurements along the length of the TC cable. For this application, the number of severe thermal transients due to rapid startup/shutdown should be kept below five.

See Table 2 for a summary of the HTIR-TC general requirements.

Continued on next page

Continued from previous page

References

[1] Dayal, Y., Jensen, C. 2019. "Guidelines for Developing and Qualifying Instrumentation Systems at Idaho National Laboratory," Idaho National Laboratory, GDE-947 Rev 0.

[2]. Skifton, R. 2021. "High Temperature Irradiation Resistant Thermocouple Qualification Requirement Report," Idaho National Laboratory, INL/EXT-21-63269.

[3] Skifton, R. 2021. "High Temperature Irradiation Resistant Thermocouple Preliminary Design Report," INL/INT-20-60511, Idaho National Laboratory, INL/EXT-21-63198.

[4] Skifton, R. 2021. "High Temperature Irradiation Resistant Thermocouple Preliminary Calibration Report," INL/INT-20-60512, Idaho National Laboratory, INL/EXT-21-63172, 2021

[5] Palmer, A.J. 2017. "HTIR Thermocouples for AGR-5/6/7," Idaho National Laboratory, SPC-1963, Rev 3.

[6] Skifton, R. 2021. "High Temperature Irradiation Resistant Thermocouple Function and Operation Report," Idaho National Laboratory, INL/EXT-21-63173.

[7] Scates, D., Reber, E.L., Miller, D. 2020. "Fission gas monitoring for the AGR-5/6/7 experiment," Nuclear Engineering and Design, 358. https://doi.org/10.1016/j.nucengdes.2019.110417.

[8] T Pham, C.B., Sterbentz, J.W., Hawkes, G.L., Scates, D.M. Palmer, J. 2020. "AGR-5/6/7 Experiment Monitoring and Simulation Progress," INL External Report, INL/EXT-19-55429. https://www.osti.gov/servlets/purl/1689160.

Fuel Refabrication Capabilities

Joe Palmer
Idaho National Laboratory

Kory Manning
Idaho National Laboratory

Introduction

For decades, the Halden Boiling Water Reactor (HBWR) in Norway was a key resource for assessing the behavior of nuclear fuels and materials in order to address performance issues and answer regulatory questions. Halden's contributions to modern global light-water reactor (LWR) technologies have been expansive and crucial to the nuclear industry, which faces decreasing financial resources and fewer available test facilities. With increasing technical, financial, and political challenges, the HBWR has ceased operations and will undergo decommissioning, thus entailing the loss of significant experimental capabilities for prototypical irradiation testing. This loss represents a great challenge, as well as an opportunity for the reactor fuels R&D community to fill in the resulting capability gaps and thus sustain the current LWR fleet while continuing to further the development of advanced LWR technologies.

The Halden Reactor Project (HRP) was renowned for its success in conducting online in-pile measurements under prototypic LWR conditions. The success of the HRP online instrumentation was closely linked to the HRP's capability to remanufacture, equip, and repair/refurbish instrumentation on pre-irradiated fuel rods, many of which came from commercial power reactors. This approach provided access to data on specific fuel specimens of interest, and these data included the state of the fuel at nearly any point in its lifetime.

To avoid losing the unique experimental techniques developed at Halden, Idaho National Laboratory (INL) procured a set of three equipment modules designed to instrument irradiated sections of LWR fuel rods prior to re-inserting them into a test reactor. This project increases the capability to deploy and demonstrate advanced in-core instrumentation, contributing to the broader effort to transfer technology and expertise developed at Halden to Department of Energy facilities. This approach to fuel testing is key to advancing and qualifying new LWR technologies.

Refabrication Process

Fuel refabrication typically starts with cutting out a 150-400 mm length of irradiated fuel. This length is then transferred to the defueling station, which is essentially a purpose-built milling machine. The defueling system is used to remove one fuel pellet from each end of the shortened rod (now referred to as a rodlet), and to remove oxides from the cladding surfaces prior to welding.

The rodlet is then transferred to a cryogenic drilling station. The rodlet is immersed in liquid CO_2, which is then solidified using liquid nitrogen. This stabilizes the irradiated fuel pellets as a hole is drilled through the center of several of them, enabling installation of a thermocouple or other type of sensor.

After the thermocouple and end fittings are installed, the rodlet is transferred to the welding station, where the end fittings are seal welded in place and a helium leak check is performed on the completed assembly.

Figure 1. Defueling module removing first pellet from one end of a prototype fuel rod.

Looking Forward

The approach to fuel rod refabrication is an essential ingredient for the successful collection of high-value data in irradiation tests. This new capability enables testing to be conducted on fuels brought in from commercial reactors to serve a variety of experimental needs. This capability allows fuel rods from nearly any source or level of burnup to be fashioned into

Continued on next page

Continued from previous page

a form that is amenable to insertion into irradiation test rigs. The re-instrumentation capability allows fuel measurements to be taken at any stage of the fuel's lifetime, alleviating the high burden placed on instrument technology to survive the lifetime of fuel to high burnups. For example, the fuels may originate from a commercial power plant or long-term irradiation experiment at any level of burnup. The rod can be remanufactured to the desired length while installing sensors, then reinserted into a steady-state irradiation environment or a transient test (e.g., a loss of coolant accident) where measurements may be taken regarding the current state of the fuel.

Thermocouples were the primary type of instrumentation utilized for temperature measurement in the HBWR (especially for centerline measurements within the fuel). Additionally, linear variable differential transformer (LVDT) sensors for measuring fuel temperature (expansion thermometer), fuel rod plenum pressure, and cladding/fuel elongation were installed within fuel rods, along with a differential transformer for measuring rod diameter. The same techniques employed for installing thermocouples in fuel rods are also employable for installing gas flow lines to allow for online fission product monitoring, or to enable active control of the gas composition in a fuel rod.

Figure 2. Drilling module starting to drill a 2.5 mm hole 50 mm deep into a fuel pellet stack (in preparation for installing a thermocouple)

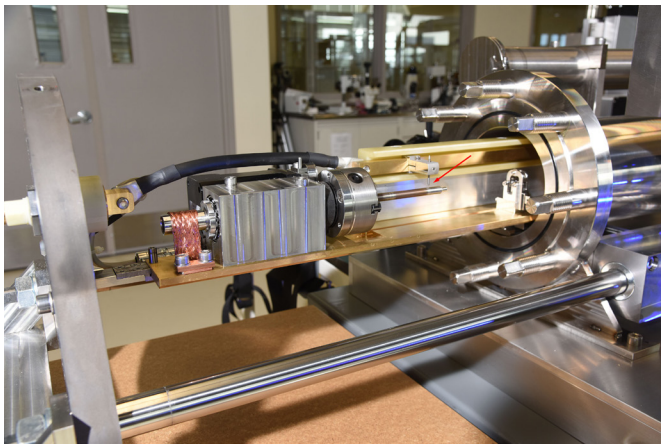

Figure 3. Prototype fuel rod installed in welding chamber with tungsten electrode positioned for welding

Applications of Laser Ultrasonic Sensing to Nuclear Applications

Bradley Bobbs
Intelligent Optical Systems

Marvin Klein
Intelligent Optical Systems

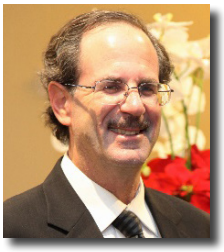

Introduction

Laser ultrasonic sensing (LUS)[1] uses the same basic principles as conventional ultrasonic sensing, but using two lasers instead of transducers to generate and detect ultrasonic pulses. This gives it advantages – e.g., avoiding contact with very hot surfaces, exceptional spatial resolution, the capability to fit into tight spaces and move quickly from one place to another, and, when using unique receivers developed by Intelligent Optical Systems (IOS), the ability to work on curved, rough, and mechanically noisy surfaces—that can be critical in certain applications.

A basic LUS system is shown schematically in Figure 1. A pulsed, high-energy laser beam is focused onto the sample surface, generating an ultrasonic pulse that propagates into the sample, interrogates some feature of interest, and returns to the surface. The resulting surface displacement is sensed by a separate continuous-wave (CW) detection laser and interferometric receiver. Commercial factory-qualified receivers developed at IOS have been adapted for optical fiber connections and enhanced for operation on rough surfaces and in harsh environments.

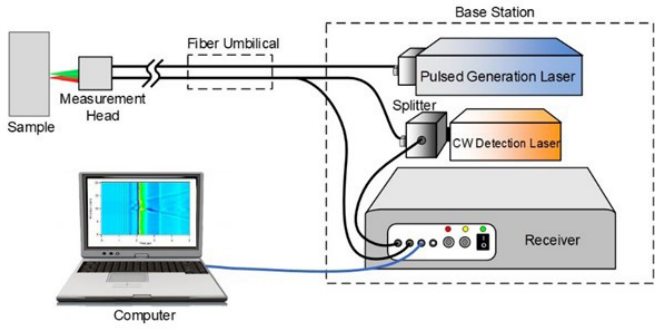

Figure 1: Basic laser ultrasonic sensing system layout.

Non-invasive Flow Monitoring

Advanced nuclear reactor technology currently being developed with improved safety, cost, sustainability, and safeguard ability, e.g., the Gen IV molten salt reactor[2], use chloride or fluoride salts for both dissolved-fuel delivery and cooling. Accurate flow measurement of the molten salts will be required initially for test purposes, and eventually for monitoring operating reactors, and must be non-invasive to avoid disturbing the flow or reactor operation. The operating temperature, up to 725°C, is too high for any current non-invasive flowmeters, but not for non-contact LUS.

Figure 2 illustrates our concept for a non-invasive LUS flowmeter. Two probes, each having both generation and detection laser beams, measure both upstream and downstream shifts in ultrasonic pulse arrival times. Subtracting these time shifts compensates for errors due to thermal and all other environmental changes, yields high flow sensitivity. This concept has been demonstrated in our laboratory, with a correlation between LUS time difference signal and known flow speed shown in Figure 3.

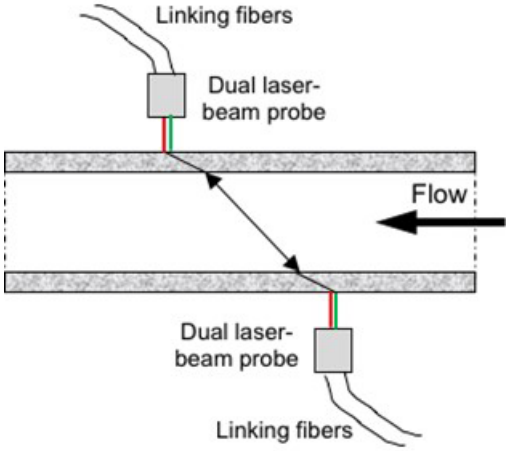

Figure 2. IOS concept for laser ultrasonic flow sensing, showing cross-section through a flow pipe.

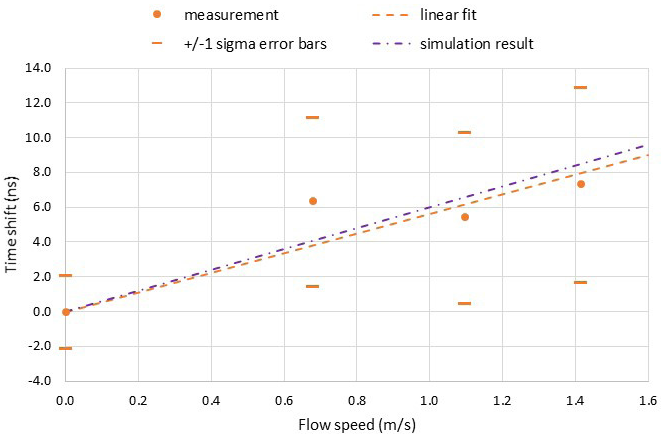

Figure 3. Correlation between LUS time difference signal and known flow speed.

Continued on next page

Crack Depth Profiling in Nuclear Waste Canisters

The stainless-steel canister inside a dry cask storage system (DCSS) for spent nuclear fuel rods is at risk for chlorine-induced stress corrosion cracking, especially at storage sites exposed to salt-rich climates. A viable technique for in-situ nondestructive evaluation of cracks is needed to determine when corrective measures must be taken.[3,4]

Figure 4 shows our LUS configuration to determine crack depth profile, with generation and detection laser beams positioned on opposite sides of the crack, and scanning together along the crack length. Among the ultrasonic waves produced by the generation laser are surface Rayleigh waves and longitudinal (L) waves that propagate into all directions below the surface. When no crack is present, a skimming L-wave just below the surface travels directly to arrive at the detection beam and be detected there. When a crack is present an L-wave travelling at an angle to the surface will diffract or scatter from the tip of the crack, and part of it will return to the surface at the detection beam.

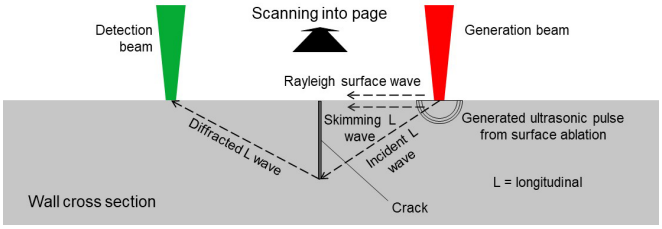

Figure 4. Cross-section through a canister wall, showing LUS configuration to determine crack depth profile.

Figure 5 shows an example LUS "B-scan" of position along a crack vs. arrival time of the ultrasonic pulse, as measured in our laboratory on a known test crack. Overlaid onto the B-scan is a line determined by our digital near-real-time tracking algorithm, which converts directly to crack-depth profile. This was found to be consistent with the known crack profile, and with profiles measured for different laser beam separations.

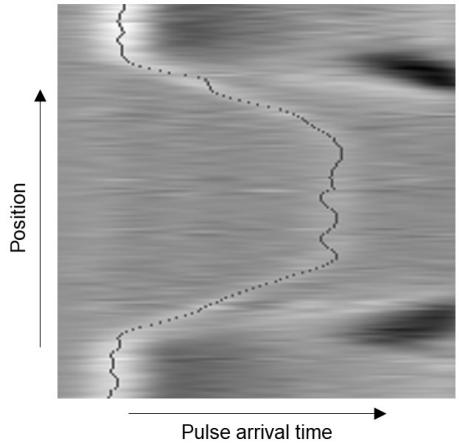

Figure 5. Laboratory LUS B-scan, overlaid with a dotted line for crack profile determined by our near-real-time tracking algorithm.

We designed a compact LUS measurement probe head integrated onto a robotic crawler to go into the tight access spaces of a DCSS. Figure 6 shows the probe being mechanically tested inside a DCSS mockup at Pacific Northwest National Laboratory.

Figure 6. LUS probe being mechanically tested inside a DCSS mockup. Left: entering access vent. Right: inside vertical 2" annular space between canister and concrete overpack wall.

Measuring Internal Pressure and Wall Thickness of Nuclear Fuel Rods

Nuclear fuel rods can develop cracks, pinholes, and other defects causing leakage, which can lead to a loss of pressure and water ingress. Release of fission gas, particularly under high burnup conditions, can lead to dangerous levels of overpressure. Changes in rod cladding wall thickness can indicate cladding corrosion or oxide layer buildup. It is essential that any of these indications of rod integrity degradation be detected during period maintenance in a cooling pool. Using conventional ultrasonic for this is considered to be only ~60% reliable.[5] Eddy current and gamma scanning measurements are more reliable, but require that rods be laboriously removed from their array assembly.

In our LUS technique, a pulsed generation laser excites resonant frequencies of the fuel rod, and a detection laser measures a temporal response that is Fourier-transformed to yield those frequencies. Figure 7 shows a laboratory measurement of a surrogate rod immersed in water. Internal pressure and cladding wall thickness of the rod can be determined from the resonant frequency shifts; but only after applying a self-referencing algorithm we

Continued on next page

Continued from previous page

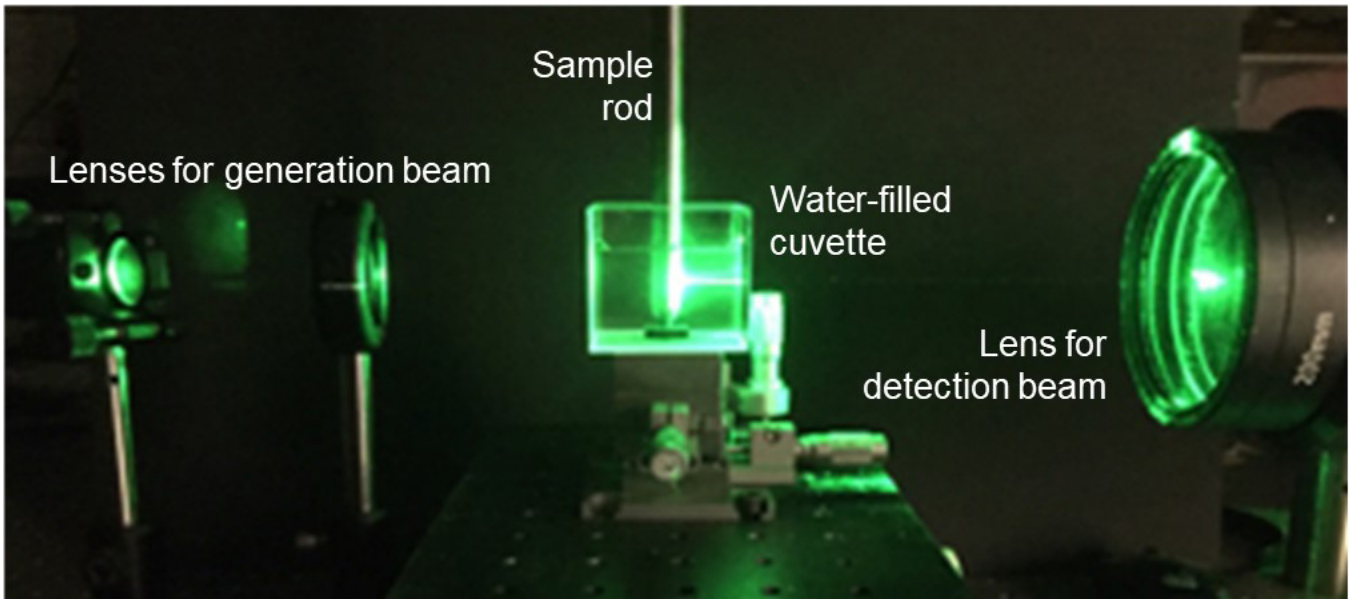

Figure 7. Laboratory LUS measurement of a surrogate rod immersed in water.

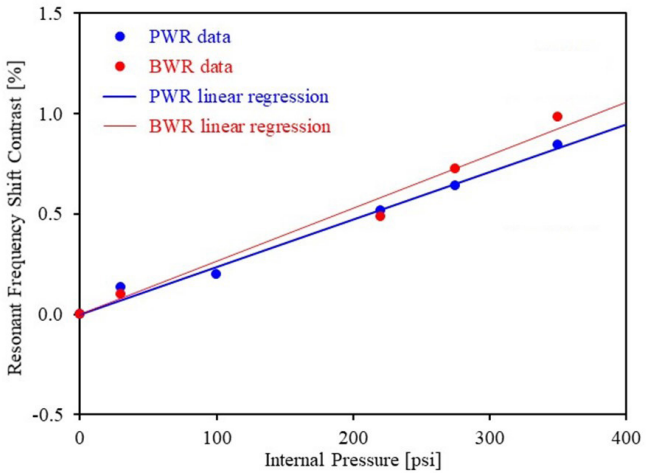

Figure 8. Measured pressure dependence of an error-compensated frequency shift parameter for PWR and BWR types of rods.

developed to compensate for relatively large rod-to-rod and time-dependent random variations. Figure 8 shows the determined pressure dependence of an error-compensated frequency shift parameter for two types of rods.

Our development of this technique continues with enhanced theoretical simulations, laboratory demonstrations, and error-compensating algorithms that consider both fill gas and fusion-generated gas; design of a miniaturized LUS probe for use inside a rods array without requiring disassembly; and planning for in-situ testing in a research cooling pool.

References

[1] C.B. Scruby and L.E. Drain, Laser Ultrasonics: Techniques and Applications, Adam Hilger, Bristol, 1990

[2] U.S. Nuclear Energy Research Advisory Committee and the Generation IV International Forum, "A technology roadmap for Generation IV nuclear energy systems," GIF-002-00, December 2002, https://www.gen-4.org/gif/upload/docs/application/pdf/2013-09/genivroadmap2002.pdf, accessed 3/15/2022

[3] X. He, et al., "Available methods for functional monitoring of dry cask storage systems," Prepared for U.S. Nuclear Regulatory Commission under Contract NRC–HQ–12–C–02–0089, November, 2014

[4] M. Lombard, "NRC: No technology to find cracks in Holtec thin nuclear waste canisters," https://www.youtube.com/watch?v=QtFs9u5Z2CA, accessed 3/15/2022

[5] Tom Morello, Exelon Corp., private communication, Apr. 12, 2021

Advanced In-Core Neutron Detection through Machine Learning

J. Thomas Gruenwald:
Blue Wave AI Labs LLC

Jonathan Nistor
Blue Wave AI Labs LLC

Jordan Heim
Blue Wave AI Labs LLC

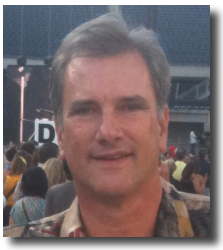

Introduction

Recent trends in the nuclear industry have focused on advancing the online monitoring capabilities of plant components and processes, resulting in the collection and retention of vast amounts of plant data. There is a clear opportunity to apply artificial intelligence (AI) and machine learning (ML) to improve nuclear power plant (NPP) efficiency and reduce costs. Machine learning is a branch of AI focused on learning from data, extracting information, and gaining deeper insights into complex relationships. Its applications are incredibly diverse, including things such as computer vision, fraud detection, cyber intrusion, and analyzing MRI and CT scans. AI can be used over a wide range of nuclear plant operations, from predicting component lifetimes and evaluating asset health to understanding core dynamics for more accurate reload planning and more favorable fuel cycle economics. In fact, the application of AI/ML to reload core design has been a key player in reducing reload fuel costs, which account for 20 percent or more of total power generation costs [1].

Under an award from the Department of Energy [2], we are working to improve the diagnostic and prognostic capabilities of nuclear power plant assess through artificial intelligence. The capabilities being developed under this project directly benefit the industry's push for increased operational efficiencies and reductions in operations and maintenance (O&M) costs. The development of enhanced prognostic and diagnostic tools will enable adoption of predictive maintenance (and health management) strategies—as opposed to more labor- and capital-intensive periodic maintenance —while improving offline methods for reliably forecasting online behavior.

Background and Motivation: In-core Neutron Flux Instrumentation

During this project, in-core nuclear instrumentation has been identified as high-value components for analysis in boiling water reactors (BWRs). Local Power Range Monitors (LPRMs) are used for in-core neutron flux measurements and perhaps constitute the most fundamental array of instrumentation within the nuclear plant—since they provide the only direct means for determination of the radial, bundle, and nodal power distributions. These quantities are used to monitor and track metrics, such as fuel exposures and thermal limits, which must be met to ensure a safe and economically viable fuel cycle.

The array of LPRMs consist of up to 172 individual detectors distributed among 43 instrument tubes within the reactor core, as shown in Figure 1. Each instrument tube houses a string of four detectors that are situated

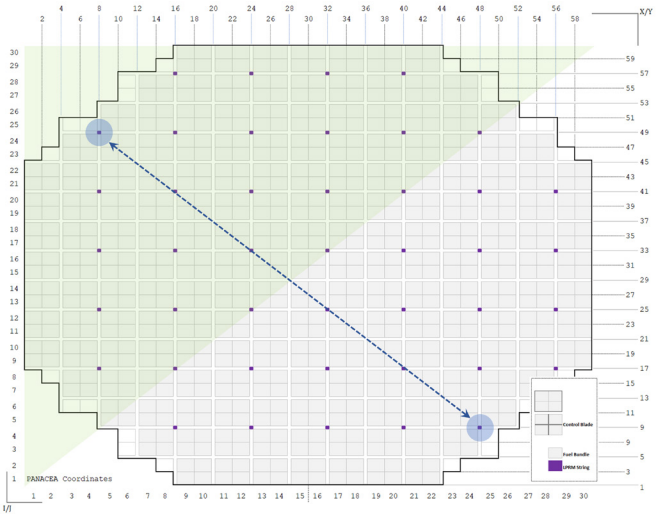

Figure 1: Top-view layout and distribution of LPRM strings (and instrument tubes) in a large 30-by-30 BWR core. The core exhibits a symmetry axis (lower-left to upper-right) with respect to the placement of the instrument tubes. LPRM symmetric partners should exhibit similar behavior for a symmetrically designed core (early in the cycle before any asymmetric burn occurs). This provides a valuable benchmark for assessing the baseline performance of the ML models trained.

axially from top to bottom of the core. LPRMs exhibit response degradation over their lifetime (many years) due to the depletion of incorporated uranium isotopes which are necessary for their operation. Each detector's exposure is tracked and forecasted, and regular calibrations are performed (approximately every two months) with traversing in-core probes (TIPs). These

Continued on next page

Continued from previous page

probes are inserted through the instrument tubes and withdrawn at a fixed rate to produce a "trace" of the axial power along each LPRM string. The traces are, first, adjusted to align with proper vertical positioning within the core, and then used to adjust the LPRMs to account for the loss in their sensitivity since the prior calibration.

Our utility partners have cited several issues surrounding the LPRM system: (1) The four LPRMs per string must all be replaced at once, typically when one or more are expected to reach their end-of-life (EOL), which is costly. (2) Various failure modes may cause spurious high- or low-alarm behavior and require manual bypassing of the offending detector until replacement, reducing visibility into the operational state of the core. (3) Calibration of the detector array is demanding and required approximately every two months. Moreover, (4) the alignment and calibration process, itself, is susceptible to gross inaccuracies that can cause erroneous thermal limit calculations, resulting in millions of dollars in wasted capacity. Finally, (5) the LPRM decay model is simplistic and outdated, resulting in wasted resources, premature replacement, or overestimation of a detectors remaining useful life.

Virtual Calibration & Virtual Measurements via Machine Learning

Leveraging the underlying relationships among the LPRMs with historical operating data from our utility partners has presented a tractable path to enabling virtual measurement capabilities for the array of LPRMs. This will provide a means for (i) virtual calibrations, thereby reducing the necessary interval between successive TIP calibrations, (ii) more accurate prediction of EOL that will enable utilities to reduce the number of LPRMs that are replaced prematurely, and (iii) more reliable determination of nodal powers and thermal limits, both online and at the design stage, that will reduce a costly bias associated with additional margin to account for current uncertainty.

From our utility partners, we have obtained a vast amount of data spanning the past twenty years at 9 reactor units. These datasets (totaling over 50 gigabytes) consist of operational plant data, LPRM measurements, TIP traces, outputs from core monitoring systems and core simulators, event log reports, maintenance logs, configuration data, replacement summaries, EOL determination worksheets, and the like. In the context of supervised machine learning, this amounts to tens of thousands of training samples (features plus targets) for each reactor unit. From this information, three types of models have been developed, characterized by the nature of the data used as model inputs and the intended application for the model:

- **Type 1** predicts the reading of any given LPRM, using readings from other LPRMs as model inputs. The advantages of this model are to enable real-time virtual readings (which can be used as redundancy when an LPRM goes offline or is bypasses), to provide a means for virtual calibration, and to detect anomalies for real-time diagnostic health assessment.
- **Type 2** predicts the array of LPRM readings from core conditions and cycle parameters that are obtained through a core simulator. The primary added benefit of this model is the ability to forecast LPRM behavior into the future from inputs that are readily projected during core design and cycle management processes. By removing the "online" LPRM measurements as inputs to the model, the model becomes a reliable offline prediction system for online phenomena. Hence, this model provides a direct path to ascertaining high-fidelity remaining useful life and EOL determinations from the anticipated operating conditions in the core, as opposed to historical trending.
- **Type 3** is an error correction model that predicts the array of LPRM readings from the estimates obtained from the fuel vendor's proprietary core simulator.

For all three modeling methodologies, we observe significant performance improvement when compared to the reference model of the core simulator (refer to Figure 2) and a reduction in average uncertainty by more than four-fold. Moreover, as shown in Figure 3,

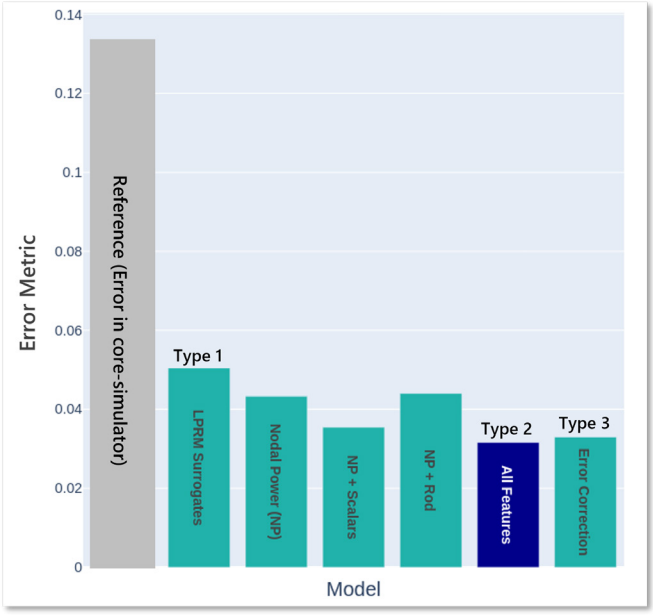

Figure 2: Performance of the three modeling methodologies (Types 1 through 3) compared to the Reference of the core simulator. The "calculated" LPRM values from the core simulator indicate an average error of approximately 14 percent (averaged across all LPRM strings and over all cycle exposures).

Continued on next page

Continued from previous page

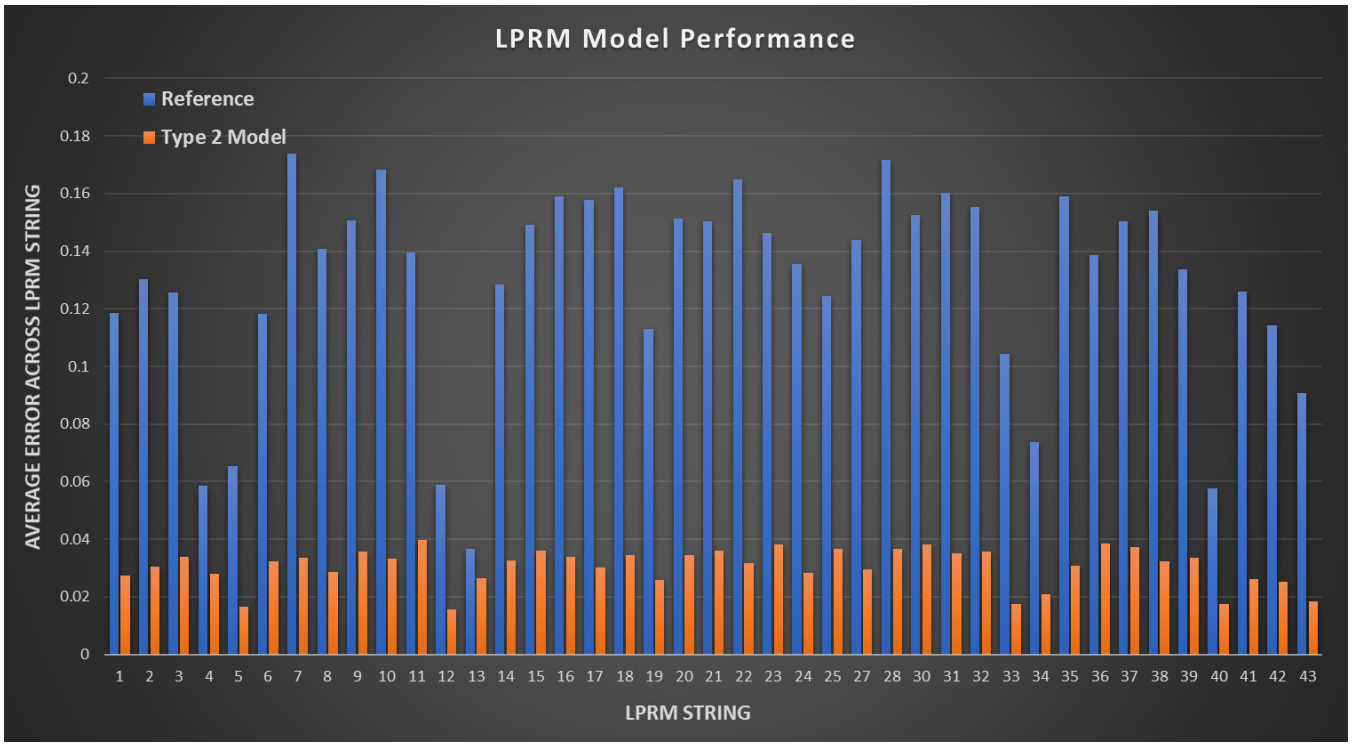

Figure 3: Performance of Type 2 models broken up by LPRM string. Unlike the core simulator, which demonstrates greater bias for some core locations, the ML models described here demonstrate similar performance across all instrument tubes and detector locations.

the model uncertainty is largely location-independent (all strings showing similar accuracies), whereas the referenced core simulator has significant regional biases within the core.

Summary & Conclusion

We have developed three distinct ML model architectures that advance the state-of-the-art and accurately predict online LPRM readings both during operation (online) and at the core design stage (offline). These models enable high-fidelity virtual measurements and virtual calibration of LPRMs, which allow for early detection of faults or degradation, on-demand calibration, accurate remaining useful life determination, and more efficient fuel reload core design.

These same models have other far-reaching applications in that they can be used to provide more precise thermal limit calculations for commenced fuel cycles, and just as important, provide unbiased thermal limit determinations for future fuel cycles from planned core conditions. All of this provides the potential for substantial operational savings and demonstrates the incredible value in applying machine learning to nuclear power generation.

References

[1] Gruenwald, J.T., J. Nistor, and J. Tusar. "Powering our Nuclear Fleet with Artificial Intelligence." Nuclear News, vol. 65, no. 02, February 2022.

[2] U.S. Industry Opportunities for Advanced Nuclear Technology Development Funding Opportunity Announcement (FOA) Number DE-FOA-0001817.

Integration of Wireless Sensor Networks and Battery-free RFID for Advanced Reactors

Faranak Nekoogar, Ph.D.
Dirac Solutions Inc.

Introduction

To address an important need for Nuclear Power Plants (NPPs) to significantly reduce the amount of the required cables for sensor data communications, Dirac Solutions Inc. (DSI) has successfully developed a novel low-cost proof-of-concept prototype of a secure wireless sensor network backbone communications system. This system combines commercially available low power, low cost XBEE wireless communications network and passive (battery-free) Radio Frequency Identification (RFID) systems to report individual sensor data and their location through the containment wall for rapid response to anomalies in nuclear facilities.

This WIreless Sensing and Locating (WISLO) system network architecture allows non-intrusive wireless collection of sensor data with the sensor's accurate location information from inside of the instrumentation or containment area with minimal need for power sources. The multi-node sensor data in the containment area is wirelessly transmitted to outside through the metal reinforced concrete walls without the need for any batteries. The WISLO system could be readily used in current reactor fleet and future advanced reactors, as well as in small modular reactors (SMR). The WISLO system is the first passive RFID-based through-containment wall data communications system and has the following advantages:

- Low-cost, regulatory approved, and commercially available components;
- Minimal dependency on batteries or wall power;
- Secure (encrypted) wireless sensor data transmission;
- Accurate sensor location information to localize points of anomaly;
- Real-time high bandwidth sensor data collection including time-series data;
- Continuous or user programmable periodical sensor data collection;
- Battery-free data transfer through containment walls.

Background

The WISLO system uses multiple wireless sensor nodes (WSN) consisting of low-cost and low-power XBEE systems using encrypted communications to transmit sensor data and their location information to a gateway node inside the containment area. The gateway node then transmits the collected data through a thick nuclear concrete wall using a small passive (battery-free) RFID tag. A commercial RFID reader from outside the wall continuously reads the data from a suite of sensors including temperature, pressure, humidity, CO_2, and TVOC. **Figure 1** illustrates the system design of the WISLO system.

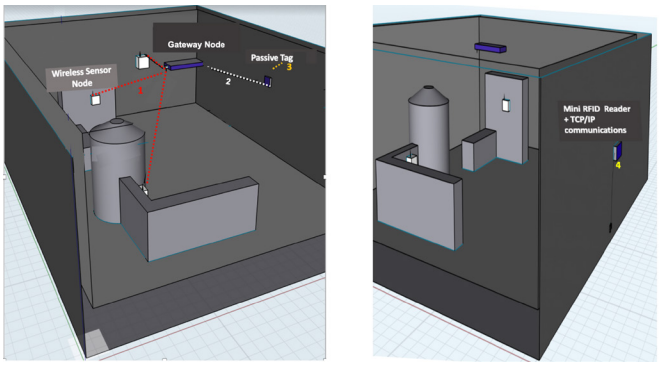

Figure 1. System design of WISLO system in NPPs allows through-concrete wireless communication system using passive RFID and sensor network technologies; the 3-4 transceiver pair constitutes the passive RFID-based through-wall communication link.

The following steps describe the role of individual components in the WISLO system shown in **Figure 1**.

1. The low cost XBEE based WSN nodes securely transmit sensor data to the gateway node;
2. The gateway node receives and processes multi-sensor data, and transfers the sensor data together with sensor locations to the passive tag (placed near or on the wall);
3. A customized passive tag designed to transfer the sensor data through the wall without the need for any batteries; i.e. data transfer through walls with only one small battery-free tag.
4. A mini RFID reader behind the wall (outside the reactor room) collects the sensor data. This data can be integrated to the NPPs central command and control computer through TCP/IP communications.

Continued on next page

Continued from previous page

All of the hardware modules in the proposed WISLO system are commercially low-cost available products. **Figure 2** shows the components of WISLO system.

Figure 2: Components of WISLO system uses sensor network nodes and passive RFID through-wall communication transceivers.

While the through-wall transceiver is fully passive, the sensor network sub-system of the WISLO also has minimal power requirements with the following low-power features:

1. Currently, the gateway node is the only device requiring wall power inside the reactor room, however, it could be equipped with an internal battery that is remotely and wirelessly activated through the concrete wall by DSI's RF remote switching/powering technology. Hence, increasing the battery life to minimum of 2 years for on demand or periodic data collection;
2. WSN nodes are battery operated and with DSI's novel battery management electronics, they can last for 2.5 years with full operational capability;
3. Passive tag is battery-free with indefinite lifetime and hardened for high doses of gamma and thermal neutron radiation.
4. The mini RFID reader outside the wall is also wall powered with a backup battery.

The WISLO system not only can modernize the sensor monitoring practices in existing reactor fleet, but also offers a secure, low-cost solution to advanced reactors and SMRs by removing cables and issues related to them such as cable integrity, reporting delays, and installation and maintenance costs. Hence improving process safety, reliability, efficiency, and cost effectiveness to the monitoring and maintenance process in current and future plants. The estimated cost for the WISLO system in quantities of mass manufacturing would be less than $5K.

Facility Tests and Results

DSI is currently finalizing its Phase I DOE SBIR effort funded by DOE Office of Nuclear Energy with successful development of WISLO system prototype. The prototype system has been tested at UC Davis McClellan Nuclear Center for through-the-wall sensor data transmission with a 24-inch nuclear concrete wall. **Figures 3 to 5** show this experiment. The system will be tested with a 3 ft and 5 ft wall prior to the end of the project.

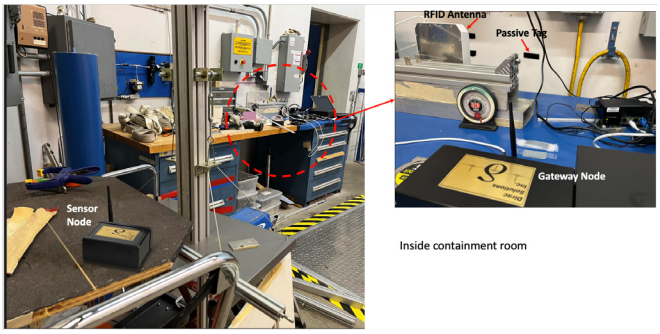

Figure 3. Inside containment room. Sensor node transmits sensor data to gateway node across the room and the small battery-free tag (size of a USB stick) transfers the data through the wall.

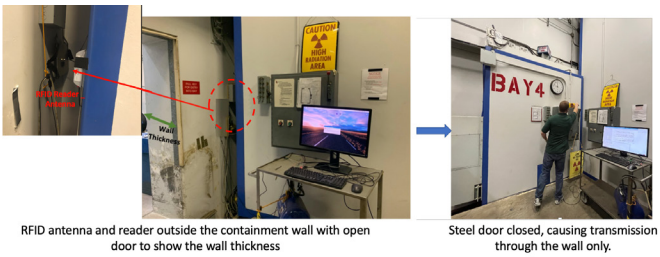

Figure 4. Outside the containment room, small RFID reader and antenna continuously monitor the inside small passive tag with steel door closed.

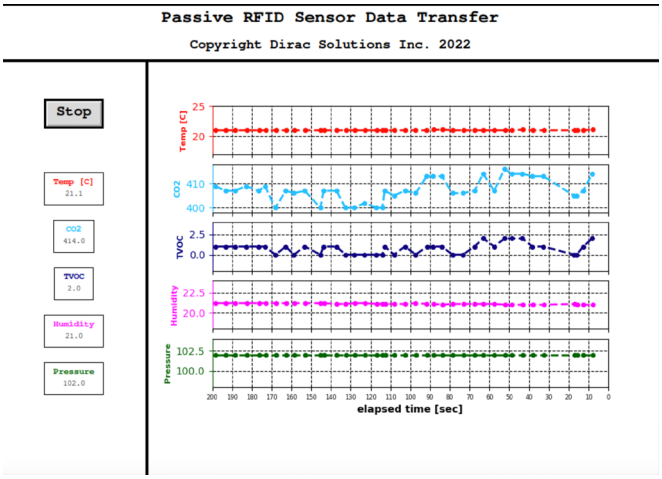

Figure 5. Graphical user interface showing time series data collected from multiple sensors inside the containment room reported by the inside small passive RFID tag through the containment wall.

Continued on next page

Continued from previous page

This set of initial field experiments conducted in the SBIR Phase I effort showed reliable sensor communications through the thick nuclear concrete wall with closed metallic doors. In Phase II, the WISLO system will be equipped with an internal battery that is activated and deactivated on demand using through-the-wall RF remote powering/ switching to remove it's dependency to the wall power, followed by final packaging including radiation hardening, low volume manufacturing, and user field evaluations. A subsequent Phase III plan will serve the needs of various wireless sensor applications of next generation and modular nuclear reactors, as well as the broad range of applications requiring secure wireless communications such as high-end commercial markets (processing plant manufacturing, semiconductor capital equipment manufacturing, etc.).

References

[1] IAEA, 2012, "Assessing and Managing Cable Aging in Nuclear Power Plants," Nuclear Energy Series No. NP-Tt3.6, IAEA, Vienna.

[2] H. Fitriawan, M. Susanto, A. S. Arifin, D. Mausa and A. Trisanto, "ZigBee based wireless sensor networks and performance analysis in various environments," 2017 15th International Conference on Quality in Research (QiR) : International Symposium on Electrical and Computer Engineering, 2017, pp. 272-275, doi: 10.1109/QIR.2017.8168495.

[3] F. Nekoogar, F. Dowla, [Book] "Ultra-Wideband Radio Frequency Identification Systems (Information Technology: Transmission, Processing and Storage)", Springer Publishing, 2011, ISBN-13: 978-144199700.

Process-Constrained Data Analytics for Sensor Assignment and Calibration

Richard Vilim
Argonne National Laboratory

Alexander Heifetz
Argonne National Laboratory

Objective

Data analytic methods are being developed to address the problem of how to assign a sensor set in a nuclear facility such that a requisite level of process monitoring capability is realized and that the sensor set is sufficiently rich to determine the status of the individual sensors with respect to need for calibration. There is an awareness in the nuclear industry that data analytics combined with rich sensor sets represent a means to improve operations and reduce costs.

In the utility industry the sensor calibration problem has been approached from an empirical data-driven perspective with several methods having been previously developed. However, the experience of the utilities over the past ten years with these methods indicates that the absence of physics-based information renders the data-driven approach less reliable. Complicating factors such as the inherent variability of operation (both equipment alignment and operating condition) can confound a pure data-driven approach while there are no rigorous guidelines for determining what constitutes an adequate sensor set.

Approach

Many of these shortcomings can be remedied by including physics in the diagnostic process. This takes the form of a digital twin which allows specific faults to be identified given an adequate sensor set. A physics-based digital twin is an analytic model constructed from first principles, which may include conservation balances and constitutive relations. It may also incorporate plant historical operating data to augment the analytic relationships and to validate them. A physics-based **digital twin** has inherent advantages over a data- driven model and is preferred when the additional development effort required is acceptable. These advantages include:

- The ability to estimate unmeasured process variables provides information that can be used to reduce sensor count through the concept of virtual sensors and allows for greater resolution of the state of a system.
- The physics-based twin can be more reliably applied outside the region of nominal calibration.

To differentiate among faults, a form of **automated reasoning** is combined with the digital twin. Automated reasoning methods provide a formal means for inferring the status of a system given a set of hypothesized relationships among system variables. Each of these relationships is individually held up for inspection as to its validity given measurements of the variables. The relationship between the process variables and fault status is given by the conservation balances for the component as represented by the digital twin.

We are using the above two capabilities to solve for the **optimal sensor set** to simplify preventative maintenance (PM) procedures. This amounts to finding a suitable population of sensors that enable a requisite degree of monitoring capability. Given a list of faults that need to be detected and isolated to a prescribed degree of spatial resolution, the algorithm finds the sensor set that will accomplish this objective at the least cost. It is an inverse problem in the sense that it is the opposite of determining what faults can be diagnosed using an existing sensor set. Instead, it determines the sensor set needed to provide a requisite fault diagnosis capability.

Current Status

The selection of an appropriate sensor set is an inverse problem whose solution is a suitable population of sensors that provide a requisite degree of monitoring capability. More specifically, given a list of faults that need to be detected and isolated to a prescribed degree of spatial resolution, find the sensor set that meets this objective at least cost. The problem is set up for solution by identifying *a priori* the required set of faults to be diagnosed and, for each component in the system, the eligible locations for sensors and, for each location, the admissible sensor types. The inverse sensor algorithm then solves for the sensor subset that yield the minimum value of a cost function.

The solution, however, suffers from the curse of dimensionality with the computation time increasing exponentially as the size of the system grows. To overcome this, we use parallel computing to reduce runtime combined with an optimization approach based on the genetic algorithm. Genetic algorithms are general purpose optimization techniques based on principles inspired from biological evolution as the "survival of the fittest". To

Continued on next page

Continued from previous page

evaluate a sensor set, the genetic algorithm calls the newly developed PRO-AID health-monitoring code [1-3] each time it spawns a new instantiation of sensors as it searches for the lowest cost set. PRO-AID provides the identity of the faults that can be resolved for a given sensor set. The graphical user interface for configuring the input to the PRO-AID software is shown in Fig. 1.

significantly widen the list of detectable faults and improve the resolution of the diagnostic results (i.e., narrow the list of possibilities in event of a fault).

Results showed that the addition of four new flowrate sensors leads to improved diagnostics. These sensors are shown in green in Fig. 2. A comparison between the diagnostic capabilities of the existing sensor set and this

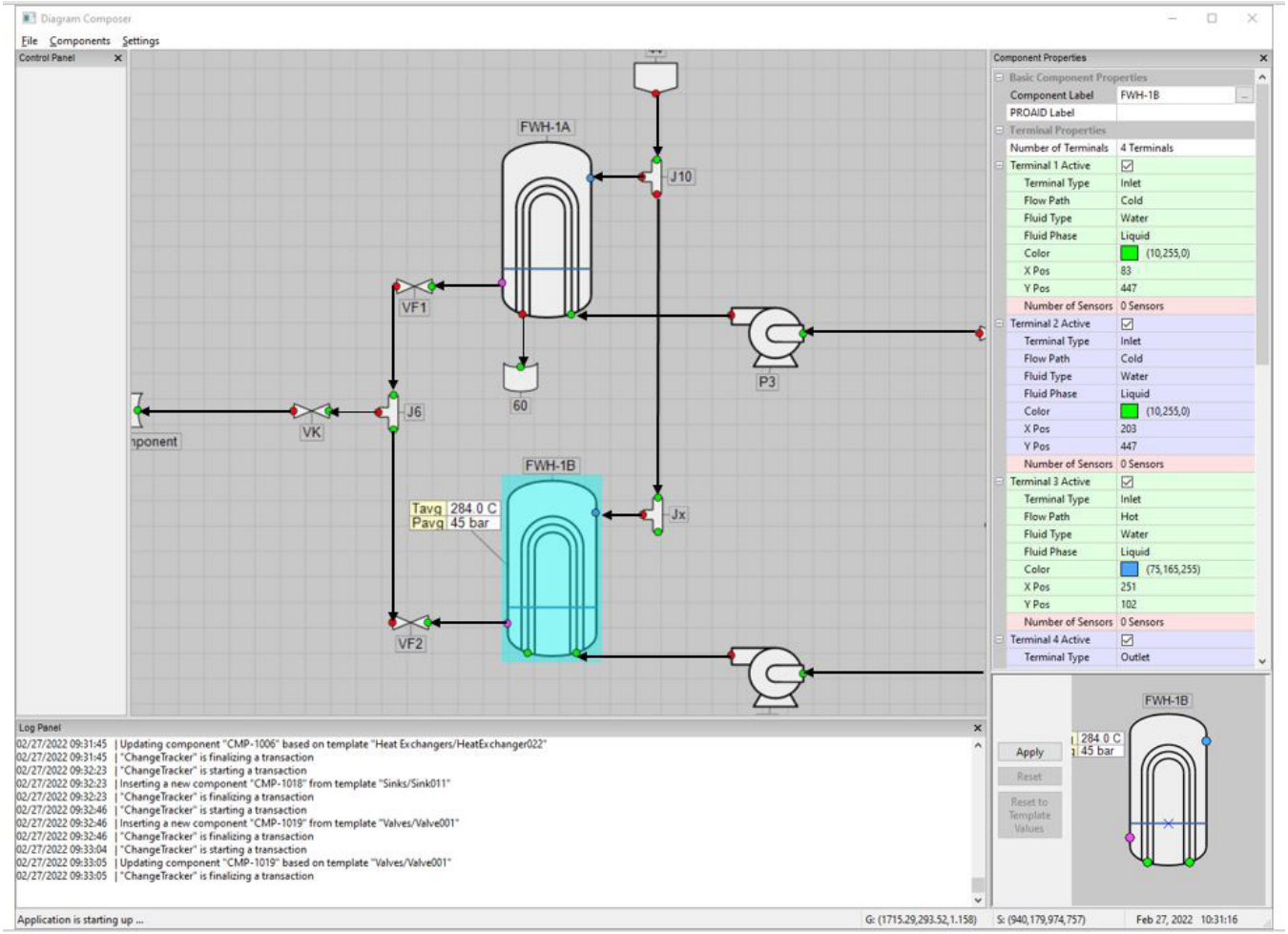

Fig. 1 Graphical user interface for configuring the PRO-AID health monitoring software

Results

The sensor set selection problem was investigated for the feedwater heater string shown in Fig. 2 of an operating boiling water reactor (BWR). We investigated the diagnostic capabilities of the existing sensor set (shown in Fig. 2) to arrive at an optimal placement of additional sensors for improved monitoring performance. The specific objective was to better detect the main faults in the five feedwater heaters, i.e., fouling and tube leakage in each of the feedwater heaters. Strategic addition of new sensors can

augmented set appears in Table 1. For most of the faults listed, the augmented sensor set allows for improved diagnostic resolution even if the faults are still not uniquely diagnosed. For example, in the event of fouling in FWH1, the diagnosis using the augmented sensor set contains three possibilities (fouling, tube leak and inlet pressure sensor fault) in comparison to four possibilities for the installed sensor set.

Continued on next page

Continued from previous page

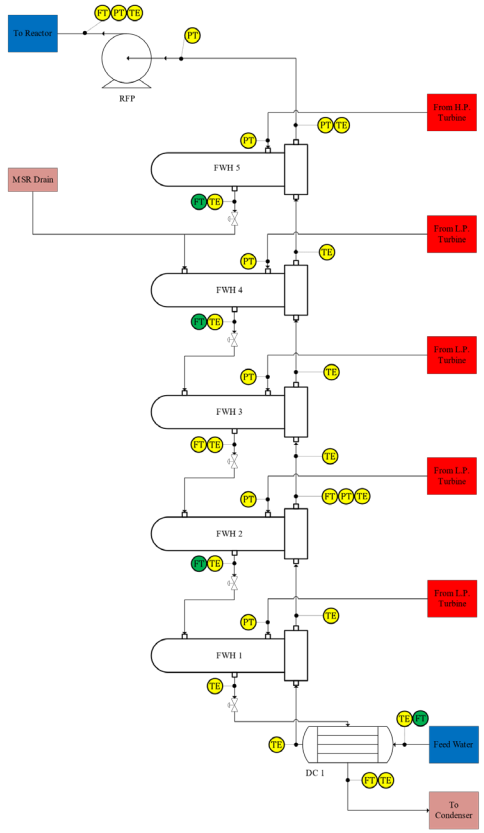

Figure 2 Augmented sensor set for BWR feedwater heater string with four new flowrate sensors (green tags)

Conclusion

We applied the methods developed in this project to solve the sensor assignment problem for the feedwater heater string of an operating BWR. The results show that greater fault resolution capability can be achieved through the addition of four flowrate sensors. This augmented sensor set provides for the detection of fouling and tube leak faults for each of the feedwater heaters in the system.

Table 1 Upgraded fault diagnostic capability for BWR feedwater heater string achieved with augmented sensor set

ID	Fault		Installed Set		Augmented Set	
	Component	Type	Detect	Uniquely Diagnose	Detect	Uniquely Diagnose
1	FWH 1	Fouling	Y	N	Y	N
2	FWH 1	Tube Leak	Y	N	Y	Y
4	FWH 1	Shell Leak	Y	N	Y	N
5	FWH 2	Fouling	N	N	Y	N
6	FWH 2	Tube Leak	N	N	Y	Y
8	FWH 2	Shell Leak	N	N	Y	N
9	FWH 3	Fouling	Y	N	Y	N
10	FWH 3	Tube Leak	Y	N	Y	Y
12	FWH 3	Shell Leak	Y	N	Y	N
13	FWH 4	Fouling	N	N	Y	N
14	FWH 4	Tube Leak	Y	N	Y	Y
16	FWH 4	Shell Leak	Y	N	Y	N
17	FWH 5	Fouling	N	N	Y	N
18	FWH 5	Tube Leak	Y	N	Y	Y
20	FWH 5	Shell Leak	Y	N	Y	N

Fouling and tube leaks are the main degradation modes contributing to reduced economic performance of the feedwater system.

References

[1] T. Nguyen, R. Ponciroli, P. Bruck, T. Esselman, J. Rigatti C, and R. Vilim, "A Digital Twin Approach to System-Level Fault Detection and Diagnosis for Improved Equipment Health Monitoring," Annals of Nuclear Energy 170, June 2022.

[2] T. Nguyen, R. Ponciroli, T. Kibler, M. Andersen, M. Strasser, R. Vilim, "A Physics-Based Parametric Regression Approach for Feedwater Pump System Diagnosis," Annals of Nuclear Energy 166, February 2022.

[3] T. Nguyen and R.B. Vilim, "A Probabilistic Model-Based Diagnosis Framework for Fault Detection and System Monitoring in Nuclear Power Plants," Annals of Nuclear Energy, 149, December 2020.